Adsorption of Bismark Brown dye on activated carbons prepared from rubberwood sawdust (*Hevea brasiliensis*) using different activation methods

B.G. Prakash Kumar, Lima Rose Miranda, M. Velan [*]

Department of Chemical Engineering, Alagappa College of Technology, Anna University, Chennai 600025, India

Abstract

Hevea brasiliensis or rubberwood tree, as it is commonly known finds limited use once the latex has been tapped. The sawdust of this tree is chosen to ascertain it viability as a precursor for activation. The carbons thus obtained were characterized in terms of iodine, methylene blue number and surface area. The best carbon in each method was utilized to study the adsorption of Bismark Brown, a dye used in the leather industry. Adsorption equilibrium studies were carried out with the synthetic solutions of the dye, at room temperature (298 K). Equilibrium data are fitted with the Langmuir and the Freundlich isotherms models for the system. The effects of contact time, adsorbent dosage and initial dye concentrations on sorption capacity were carried out. Excellent adsorption capacities of 2000 and 1111 mg g^{-1} were obtained for steam and chemical followed by steam-activated carbons, respectively. Pilot-plant experimental studies have been performed using packed-bed column with different feed concentrations, flow rates and bed heights, to evaluate sorption of Bismark Brown on steam-activated carbon. Bed depth service time (BDST) design model have been used to analyze the data.
© 2005 Elsevier B.V. All rights reserved.

Keywords: Rubberwood sawdust; Bismark Brown dye; Adsorption isotherms; Packed-bed

1. Introduction

Wastewater from textile and dyeing industries contains residual dyes, which are not readily bio-degradable are the major contributors to water pollution and poses serious threat to the environment. Increasing stringent legislation on the decontamination of wastewater has created an interest concerning the use of activated carbons for this purpose. In recent years, there has been an increasing interest in the use of lignocellulosic materials, mainly wood sawdust, as the starting material in activated carbon production by various activation methods. Activated carbon from various sources of sawdust includes beech [1], pine [2–4], yellow poplar and white oak wood [5,6], wood char [7], mahogany [8,9], medium fiber board [10], coconut tree [11], Indian rose wood [12,13], jack wood [14], sagaun [15], rubberwood [16], maple [17], mixture of wood [18], brich wood [19], *Prosopis cineraria* [20] and Babbool wood [21].

Activated carbons can be produced from carbonaceous materials, such as wood, coconut shell, anthracite, bituminous coal, etc., by physical or chemical activation. Physical activation is generally carried out at elevated temperatures between 750 and 1100 °C using oxidants, such as steam [22], carbon dioxide [23] or mixture of these gases [24]. Chemical activation is usually carried out by impregnating the precursor with activating agents, such as phosphoric acid [5,6], zinc chloride [25] and alkaline metal compounds [26,27] and pyrolyzed between 400 and 800 °C in the absence of oxygen.

Rubber tree (*Hevea brasiliensis*) is mainly grown for its latex and cut down when it becomes unproductive. These are then used as particleboards, fiberboards, packing materials and other products. To enhance the value of this bio-waste,

* Corresponding author. Tel.: +91 44 22203506; fax: +91 44 22352642.
E-mail address: velan@annauniv.edu (M. Velan).

Nomenclature

b	Langmuir constant ($L\,mg^{-1}$)
CAC	chemical-activated carbon
CC	commercial-activated carbon
CSAC	chemical followed by steam-activated carbon
C_b	allowable dye concentration at breakthrough point ($mg\,L^{-1}$)
C_e	dye concentration at equilibrium ($mg\,L^{-1}$)
C_o	initial dye concentration ($mg\,L^{-1}$)
C_t	dye concentration at time t ($mg\,L^{-1}$)
k	rate constant of adsorption ($L\,mg^{-1}\,h^{-1}$)
k_f	Freundlich constant ($mg\,g^{-1}$) $(g\,L^{-1})^n$
M	mass of the activated carbon (g)
n	Freundlich constant
N_o	adsorption capacity per volume of bed ($mg\,mL^{-1}$)
q_e	adsorption capacity at equilibrium ($mg\,g^{-1}$)
Q_o	Langmuir constant ($mg\,g^{-1}$)
SAC	steam-activated carbon
T_b	time of the dye solution treated at breakthrough (h)
V	volume of the dye solution (L)
V_b	volume of the dye solution treated at breakthrough (L)
Z	bed height (cm)
Z_o	critical bed height (cm)
ν	linear flow rate through the bed ($cm\,h^{-1}$)

preparation of activated carbon has been attempted. The objective of the present work is to study the adsorption of Bismark Brown (a cationic dye) using rubberwood sawdust (RWSD)-activated carbons prepared by various activation methods. The batch adsorption experiments were compared with commercial-activated carbon (CC). Columnar studies were carried out selecting the carbon that yielded larger BET surface area and the break through profiles were obtained. The data were analyzed using the bed depth service time (BDST) design model.

2. Experimental

2.1. Adsorbents

The carbonaceous precursor used in the study was RWSD, a bio-waste product procured from Coimbatore (India). Proximate analysis of RWSD is presented in Table 1. The RWSD was first carbonized then activated by chemical, steam or chemical followed by steam-activation processes. The description of preparation of activated carbon is summarized in Table 2.

Table 1
Proximate analysis of RWSD

Properties	wt% (wet basis)
Moisture	7.95
Fixed carbon	24.15
Volatile	62.91
Ash	4.95

2.2. Adsorbates

Bismark Brown (a cationic dye) was used for the adsorption studies. Bismark Brown R (BB) (CI 21010, $\lambda_{max} = 468\,nm$) was supplied by Ranbaxy, Mumbai, India. Double distilled water was used for the preparation of all solutions. The molecular formula of BB dye is $C_{21}H_{24}N_8 2HCl$. The structural formula of the BB dye was shown in Fig. 1. The HCl group in the structure reduces the pH towards acidic. Hence, the basic adsorbent will have more affinity for adsorption of BB dye.

2.3. Analytical techniques

Iodine number was defined as the mg of iodine per gram of carbon was determined by ASTM D 4607-86 method [28] and methylene blue number was determined by BIS 877-1977 [29] standard. The BET surface area of the activated carbons were obtained from the adsorptions of N_2 at 77 K, using Sorptomatic 1990, CE instruments. The concentration of Bismark Brown in the solution was obtained by measuring OD at 468 nm (λ_{max}) using a Hitachi UV–vis spectrophotometer (U-2000).

2.4. Batch adsorption studies

Adsorption experiments were initiated by placing a known quantity of activated carbon and 50 mL of the prepared solution into a glass-stoppered flask. The carbon loading was varied between 0.01 and 0.06 g and initial concentration between 100 and 1200 $mg\,L^{-1}$. For analysis in the linear Beer–Lambert region, the concentrated solutions were suitably diluted. The flask was placed in an orbital shaker, which was held constant at revolution of 180 cycles min^{-1}. Preliminary experiments has shown that the adsorption process attains equilibrium in 7 h for the activated carbons in the present study. Dye concentrations in the supernatant solutions were estimated by measuring the absorbance at maximum wavelengths of dyes using UV–vis spectrophotometer. The
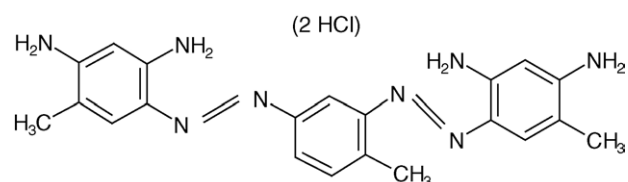

Fig. 1. The structural formula of the Bismark Brown R dye.

Table 2
Description of the production of activated carbons from RWSD

Carbon type	Process description
Chemical activation carbon (CAC)	The char was impregnated with phosphoric acid of 0.45 IR (g phosphorous: g precursor) and activated in fixed bed at $400\,^{\circ}$C for 1 h
Steam-activation carbon (SAC)	The char was activated in a fluidized bed reactor at $750\,^{\circ}$C for 1 h with steam flow rate of $4\,\text{mL min}^{-1}$
Chemical followed by steam carbon (CSAC)	The char was impregnated with phosphoric acid (0.45) IR and activated in a fluidized bed at $800\,^{\circ}$C for 1 h with steam flow rate of $5\,\text{mL min}^{-1}$

equilibrium adsorption capacities (q_e) at different solute concentrations were determined according to mass balance of the adsorbate (Eq. (1)):

$$q_e = \frac{(C_o - C_e)V}{M} \tag{1}$$

where C_o and C_e are the initial and equilibrium concentrations of the dye (mg L^{-1}), respectively, V the volume of the aqueous solution (L) and M is the mass of activated carbon used (g) in the adsorption.

The pH of the solution was varied using HCl or NaOH depending upon the required pH. It was observed that addition of NaOH caused a precipitate to be formed while addition of HCl to the solution changed the color of the solution visibly. Hence, it was necessary to carry out the batch and column adsorption studies at the solutions natural pH ($\approx$4.5).

2.5. Column studies

A glass column of 30 cm height and 1.8 cm internal diameter was used to carry out the column studies. The column was packed with the steam-activated carbon (SAC); care was taken to avoid air entrapment. The adsorbate was pumped upflow through the bed using a peristaltic pump. Experiments were carried out varying flow rate (5, 10 and 15 mL min^{-1}), the height of the packed-bed (5, 10 and 15 cm) and dye concentrations (100, 200 and 300 mg L^{-1}).

3. Results and discussion

3.1. Characterization of prepared carbons

The resulting chemical-activated carbon (CAC) and chemical followed by steam-activated carbon (CSAC) samples were washed till the pH of the carbons was neutral and SAC was found to be pH 8.0. These carbons were characterized by their iodine, methylene blue numbers and BET surface area are presented in Table 3.

3.2. Effect of contact time

Sorption of BB dye on the various activated carbons prepared from RWSD was studied as a function of contact time in order to determine the equilibrium time for maximum adsorp-

Table 3
Characterization of RWSD-activated carbons prepared by various methods

Carbon type	Iodine number (mg g^{-1})	Methylene blue number (mg g^{-1})	S_{BET} (m^2 g^{-1})
CSAC	1052	375	954
SAC	765	255	1092
CAC	835	255	822
CC	850	210	1095

CSAC, chemical followed by steam-activated carbon; SAC, steam-activated carbon; CAC, chemical-activated carbon; CC, commercial-activated carbon.

tion (Fig. 2). Nearly, 120 min for SAC, CAC and CC and 300 min for CSAC are required for equilibrium adsorption for BB dye. Therefore, the equilibrium time was set conservatively at 7 h for all the experimental runs. From Fig. 2, it was observed that the sorption capacity is very fast initially for the activated carbons except CSAC.

3.3. Effect of initial concentration

The effect of initial concentrations of the dye solution on the amount of BB dye adsorbed was studied. 0.05 g of activated carbon samples was added to each 50 mL volume of BB dye solution. The initial dye concentrations were varied between 100 and 1200 mg L^{-1}. The experimental results of sorption of BB on various activated carbons at various concentrations are shown in Fig. 3. The sorption capacity at equilibrium increases from 100 to 1456, 1085 mg g^{-1} with an increase in the initial concentration from 100 to 1200, 1600 mg L^{-1} for SAC and CSAC, respectively. The sorp-
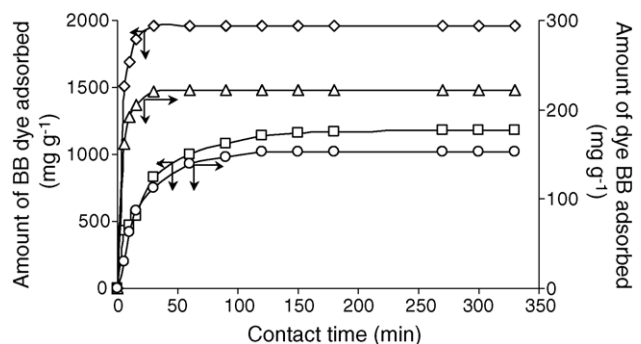

Fig. 2. Effect of contact time on the removal of BB dye from various activated carbons from RWSD. *Conditions:* 20 mg carbon dosage; SAC and CSAC 1200 mg L^{-1} dye concentrations; CC and CAC 100 mg L^{-1} dye concentrations; ($\Diamond$) SAC; ($\square$) CSAC; ($\triangle$) CC; ($\bigcirc$) CAC.
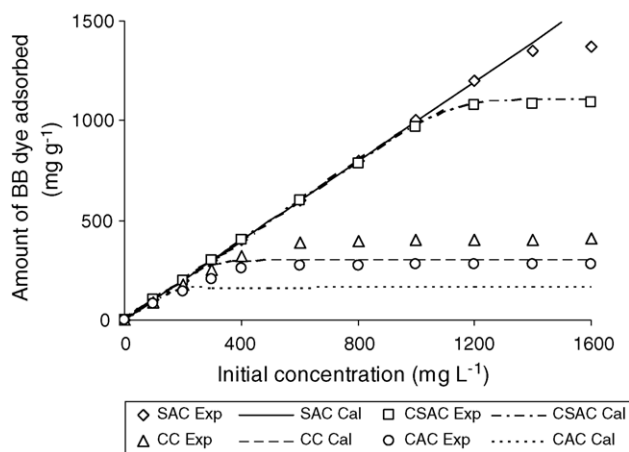
Fig. 3. Effect of initial concentration on the removal of BB dye from various activated carbons from RWSD. *Conditions:* carbon dosage, 50 mg; Exp, experimental; Cal, calculated.

tion capacity at equilibrium increases from 89 to 390 mg g^{-1} and from 79 to 271 mg g^{-1} with an increase in the initial concentration from 100 to 600 mg L^{-1} for CC and CAC, respectively. It is clear that the sorption capacity of BB dye is higher for SAC and CSAC when compared to CC and CAC. For SAC and CSAC carbons 1200 mg L^{-1} of dye concentration and for CAC and CC carbons 100 mg L^{-1} of dye concentration were chosen for further studies. The theoretically calculated amount of BB dye adsorbed by varying initial concentrations using Langmuir and mass balance equations are shown in Fig. 3.

3.4. Effect of adsorbent dosage

The effect of adsorbent dosage on BB dye uptake was investigated by varying the adsorbent dose for various activated carbons. It was observed that increase in adsorbent dosage, sorption capacity decreases as shown in Fig. 4.
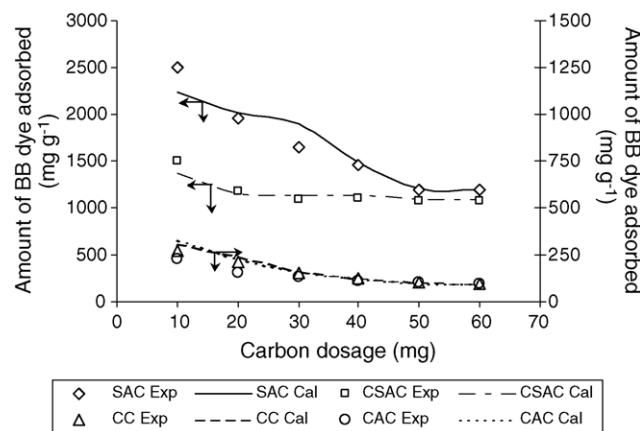

Fig. 4. Effect of carbon dosage on the removal of BB dye from various activated carbons from RWSD. *Conditions:* SAC and CSAC 1200 mg L^{-1} dye concentrations; CC and CAC 100 mg L^{-1} dye concentrations; Exp, experimental; Cal, calculated.

Decrease in sorption of 2500–1195, 1500–1072, 275–98 and 225–97 mg g^{-1} for SAC, CSAC, CC and CAC for 10–60 mg of carbon dosage, respectively. Similar results were observed by Garg et al. [12] and Banat et al. [30] for methylene blue dye adsorption by Indian rosewood sawdust and date pits, respectively. The theoretically calculated amount of BB dye adsorbed by varying carbon dosages using Langmuir and mass balance equations are shown in Fig. 4.

3.5. Adsorption models

To facilitate estimation of the adsorption capacities the two well-known equilibrium adsorption models, Freundlich and Langmuir, were employed. The Freundlich equation is an empirical one and the Langmuir equation assumes the maximum adsorption occurs when the surface is covered by the adsorbate. The Freundlich model [1,8,9,30], which is an indication of surface heterogeneity of the sorbent, is given by the following linearized Eq. (2):

$$q_e = k_f C_e^{1/n} \tag{2}$$

Eq. (2) can be rearranged to linear form:

$$\log q_e = \log k_f + \frac{1}{n} \log C_e \tag{3}$$

where k_f and n are Freundlich constants related to adsorption capacity and intensity, respectively. The values of k_f and n are in the range 54–1003 (mg g^{-1}) (g L^{-1})^n and 3.07–8.58, respectively (Table 4). Since the value of constant n is greater than unity, it indicates a favorable adsorption for all activated carbons studied.

The other model, the Langmuir equation [1,8,9,30], which is valid for monolayer sorption onto a surface with a finite number of identical sites expressed as Eq. (4):

$$q_e = \frac{Q_o b C_e}{1 + b C_e} \tag{4}$$

Eq. (4) can be rearranged to linear form:

$$\frac{C_e}{q_e} = \frac{1}{Q_o b} + \frac{C_e}{Q_o} \tag{5}$$

where Q_o is the amount adsorbed per unit mass of adsorbent corresponding to complete monolayer coverage on the surface bound at high C_e and b is the constant related to the affinity of binding sites. The values of Langmuir constants, Q_o and b are in the range of 164–2000 mg g^{-1} and 0.22–0.07 L mg^{-1}, respectively (Table 4). Using these Langmuir constants and mass balance equation, theoretical amount of BB dye adsorbed per gram of carbon were determined and compared with experimental data (Figs. 3 and 4).

The essential characteristics of a Langmuir isotherm can be expressed in terms of a dimensionless separation [1,8,9], the type of isotherm and is defined by Eq. (6):

$$R_L = \frac{1}{1 + b C_o} \tag{6}$$

Table 4
Adsorption constants for the sorption of Bismark Brown dye

Adsorbent	Freundlich			Langmuir			
	k_f (mg g^{-1}) (g L^{-1})^n	n	R^2	Q_o (mg g^{-1})	b (L mg^{-1})	R^2	R_L
SAC	1003	8.58	0.85	2000	0.07	0.98	0.012
CSAC	598	9.68	0.89	1111	0.11	0.99	0.008
CC	103	4.02	0.97	303	0.19	0.99	0.05
CAC	54	3.07	0.73	164	0.22	0.97	0.043

where b is a Langmuir constant and C_o is the initial concentration of BB dye (1200 mg L^{-1} of initial concentration of BB dye for SAC and CSAC and 100 mg L^{-1} for CAC and CC, respectively). If $R_L > 1$ unfavorable, $R_L = 1$ linear, $0 < R_L < 1$ favorable, $R_L = 0$ irreversible. Regression values (R^2) and R_L presented in Table 4 indicate that the adsorption data onto various activate carbons fitted well with the Langmuir isotherm and the adsorption is on favorable side.

It was observed that SAC and CSAC exhibit better performance for the adsorption of BB dye. These results show that one of the most important adsorption mechanisms involves the interaction between the delocalized π electrons on the carbon surface and the free electrons of the dye molecule. A similar result was observed by Pereira et al. [31].

The results showed that the performance of carbon produced in the present study was much better when compared to the results reported by Chao et al. [32] and Bhatnagar and Jain [33] for the adsorption of Bismark Brown Y on to chitosan (48.8 mg g^{-1}) and Bismark Brown R on to blast furnace sludge (85 mg g^{-1}), respectively.

3.6. Effect of bed height on packed-bed

The breakthrough curves of C_t/C_o versus time for SAC packed column for various bed heights (5, 10 and 15 mL min^{-1}) at constant flow rate of 5 mL min^{-1} and initial concentration of 100 mg L^{-1} is shown in Fig. 5. Breakthrough time (T_b) for various bed heights of 5, 10 and 15 cm a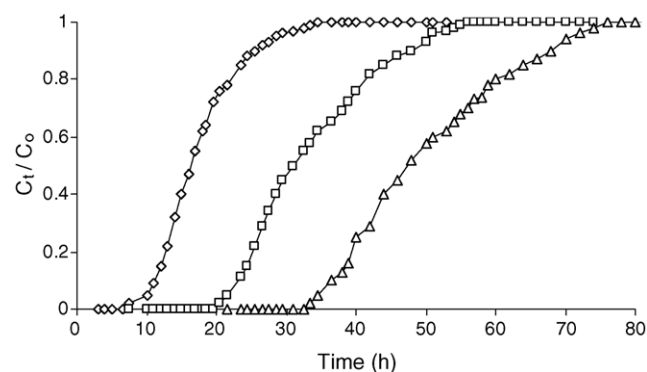re 10, 21.5 and 34.5 h, respectively. Breakthrough curve for 15 cm bed has slightly gradual curve than other bed heights. Increasing the bed height indicates a linear increase of breakthrough time.

3.7. Effect of flow rate on packed-bed

The breakthrough curves of various flow rates (5, 10 and 15 mL min^{-1}) at constant bed height of 5 cm and initial concentration of 100 mg L^{-1} is shown in Fig. 6. It can be seen that the lower flow rate (5 mL min^{-1}) has steep curve when compared to higher flow rate (15 mL min^{-1}). The T_b for various flow rates of 5, 10 and 15 mL min^{-1} are 10, 7 and 1.5 h, respectively. This clearly indicates that when increasing the flow rate, breakthrough time decreases; therefore, the volume of the dye solution treated decreases. This shows short contact time between the dye molecules and carbon adsorption sites not having enough time for diffusion. A similar trend was observed by Netpradit et al. [34].

3.8. Effect of initial concentration on packed-bed

The effect of various initial concentrations (100, 200 and 300 mg L^{-1}) of breakthrough curves at constant flow rate (5 mL min^{-1}) and bed height (5 cm) is shown in Fig. 7. Increasing the initial concentrations decreased the breakthrough time to 10, 6.5 and 4.25 h, respectively. At higher concentrations, the carbon bed is saturated within 2 h, hence, the breakthrough curve is very steep. A similar trend was observed by Walker and Weatherly [35].
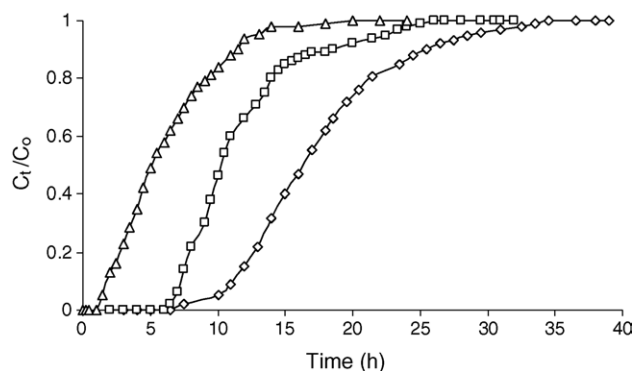

Fig. 5. Effect of bed heights on packed-bed for SAC. *Conditions:* $C_o = 100$ mg L^{-1}; flow rate, 5 mL min^{-1}; (◊) 5 cm; (□) 10 cm; (△) 15 cm.

Fig. 6. Effect of flow rates on packed-bed for SAC. *Conditions:* $C_o = 100$ mg L^{-1}; bed height, 5 cm; (◊) 5 mL min^{-1}; (□) 10 mL min^{-1}; (△) 15 mL min^{-1}.
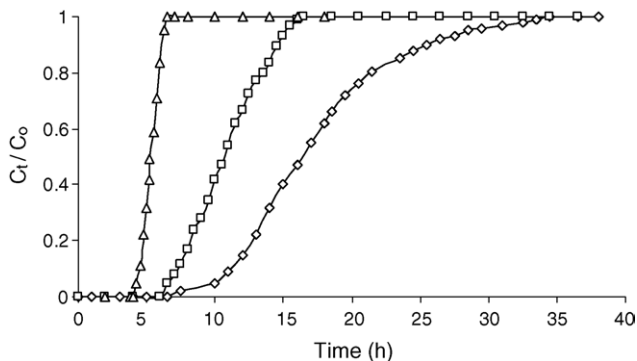
Fig. 7. Effect of initial concentrations on packed-bed for SAC. *Conditions:* flow rate, 5 mL min^{-1}, bed height, 5 cm; ($\Diamond$) 100 mg L^{-1}; ($\Box$) 200 mg L^{-1}; ($\triangle$) 300 mg L^{-1}.

3.9. BDST model

The bed depth service time model proposed by Bohart and Adams [36] and later linearized by Hutchins [37] and McKay and Bino [38] offer the simplest approach and most rapid predictions of adsorber performance. Bohart and Adams [36] proposed a relationship between the service time T_b and bed height Z:

$$T_b = \frac{N_o Z}{C_0 v} - \frac{\ln\left(\frac{C_0}{C_b} - 1\right)}{k C_0} \tag{7}$$

This equation is called the bed depth service time design model as suggested by Hutchins. Eq. (7) has the form of a straight line:

$$T_b = mZ - C \tag{8}$$

Adsorption capacity (N_o) and rate constant (k) can be found from slope (m) and intercept (Z) by plotting data on T_b versus Z. C_o and C_b are the initial concentration and desired break through concentration (5% of the inlet feed concentration) was determined. The critical bed depth Z_o can be calculated from the relationship of Eq. (7) by letting $T_b = 0$ and solving from Z:

$$Z_0 = \left(\frac{v}{kN_0}\right)\ln\left(\frac{C_0}{C_b} - 1\right) \tag{9}$$

Once the BDST relationship is established experimentally by running at least three bed heights at the same flow rate and concentrations, it is possible to predict the service times for different v (linear flow rate through the bed) from the following equation:

$$m^1 = m\left(\frac{v}{v^1}\right) \tag{10}$$

where m^1 and v^1 are the new slope value and new flow rate, respectively. Since k is not affected by a change of v, the intercept remains unchanged. For different C_o, the service
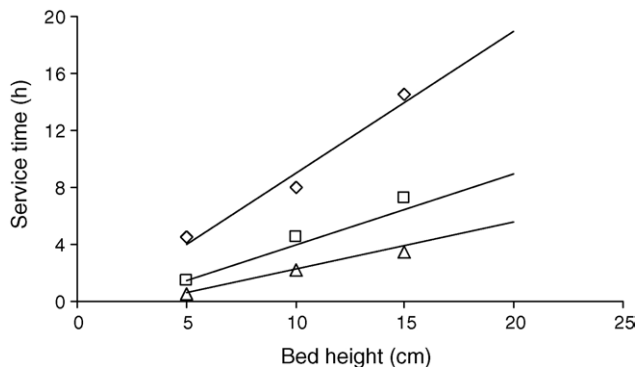

Fig. 8. BDST plots for various flow rates for SAC. *Conditions:* $C_o = 300$ mg L^{-1}; ($\Diamond$) 5 mL min^{-1} experimental; ($\Box$) 10 mL min^{-1} experimental; ($\triangle$) 15 mL min^{-1} experimental; (—) predicted.

time can be found from following Eqs. (11) and (12):

$$m^1 = m\left(\frac{C_0}{C_0^1}\right) \tag{11}$$

$$C^1 = C\left(\frac{C_0}{C_0^1}\right)\frac{\ln\left(\frac{C_0^1}{C_0} - 1\right)}{\ln\left(\frac{C_0}{C_b} - 1\right)} \tag{12}$$

where C^1 and C_0^1 are the new intercept value and new concentrations, respectively.

3.10. BDST with variation in flow rates and concentrations

Comparison of experimental and predicted service times for various flow rates at constant dye concentration of 300 mg L^{-1} and for various dye concentrations at constant flow rate of 10 mL min^{-1} on BDST model are shown in Figs. 8 and 9, respectively. The break through point for BDST calculations in this study was fixed at 5% of the inlet feed concentration. The service time obtained was maximum as low flow rate and low initial concentration. The predicted service times for various flow rates and various
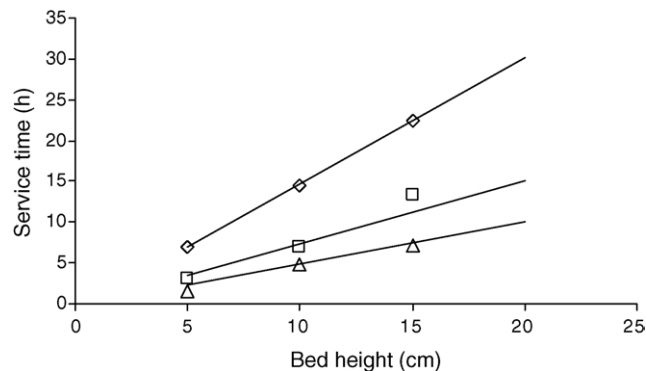

Fig. 9. BDST plots for various dye concentrations for SAC. *Conditions:* flow rate, 10 mL min^{-1}; ($\Diamond$) 100 mg L^{-1} experimental; ($\Box$) 200 mg L^{-1} experimental; ($\triangle$) 300 mg L^{-1} experimental; (—) predicted.

Table 5
Effect of flow rate on BDST model

Flow rate (mL min^{-1})	ν (cm h^{-1})	N_o (mg mL^{-1})	k (L mg^{-1} h^{-1})	Z_o (cm)	Adsorption capacity of SAC (mg g^{-1})
5	108.6	32.58	0.009	1.09	712
10	217	37.43	0.013	1.31	800
15	325.2	29.27	0.009	3.63	556

Conditions: $C_o = 300$ mg L^{-1}.

Table 6
Effect of initial concentration of dye on BDST model

Concentration (mg L^{-1})	N_o (mg mL^{-1})	k (L mg^{-1} h^{-1})	Z_o (cm)	Adsorption capacity of SAC (mg g^{-1})
100	33.64	0.035	0.54	925
200	44.49	0.005	2.87	1125
300	37.43	0.008	2.13	800

Conditions: flow rate = 10 mL min^{-1}; linear flow rate (ν) = 217 cm h^{-1}.

dye concentrations have agreed well with the experimental data (Figs. 8 and 9). The critical bed depth (Z_o), the adsorption capacity (N_o) and the rate constant (k) were calculated and shown in Tables 5 and 6. However, N_o and k did not show consistent trend for variation of flow rates and initial concentrations. For various flow rates and concentrations, the values of N_o and k is in the range of 29.27–44.49 mg mL^{-1} and 0.005–0.035 L mg^{-1} h^{-1}, respectively. The similar trend was observed by Walker and Weatherley [35], when they adsorbed the acid dyes on granular-activated carbon in a fixed bed column. The maximum adsorption capacity of BB dye on SAC by batch experiments (Table 4) is higher than the column experiments (Tables 5 and 6). This clearly indicates that the contact time between the dye solution and adsorbate were not sufficient. Therefore, the batch system provides better interaction between carbon and dye.

4. Conclusion

From the results of the present work, it can be said that: (i) the bio-waste rubberwood sawdust is efficient for the removal of Bismark Brown dye; (ii) the adsorption process follows the Langmuir isotherm, showing monolayer coverage of dye molecules at the outer surface; (iii) the adsorption capacity of Bismark Brown dye increases in the order of CAC < CC < CSAC < SAC carbons. However, steam-activated carbon has a very high adsorption capacity of 2000 mg g^{-1} when compared to commercial-activated carbon; (iv) the BDST design model is capable of describing and predicting the performance of packed-bed column in the adsorption of Bismark Brown dye using steam-activated carbon.

References

[1] F.A. Batzias, D.K. Sidiras, Dye adsorption by calcium chloride treated beech sawdust in batch and fixed-bed systems, J. Hazard. Mater. 18 (2004) 167–174.

[2] R.L. Tseng, F.C. Wu, R.S. Juang, Liquid-phase adsorption of dyes and phenols using pine wood based activated carbons, Carbon 41 (2003) 487–495.

[3] Y. Muñoz, R. Arriaganda, G. Soto-Garrido, R. García, Phosphoric and boric acid activation of pine sawdust, J. Chem. Technol. Biotechnol. 78 (2003) 1252–1258.

[4] I. Mahmut Özacara, Ayhan Şengilb, Adsorption of metal complex dyes from aqueous solutions by pine sawdust, Bioresour. Technol. 96 (2005) 791–795.

[5] M. Jagtoyen, F. Derbyshire, Activated carbons from yellow poplar and white oak by H$_3$PO$_4$ activation, Carbon 36 (1998) 1085–1097.

[6] M.S. Solum, R.J. Pugmire, M. Jagtoyen, F. Derbyshire, Evolution of carbon structure in chemically activated wood, Carbon 33 (1995) 1247–1254.

[7] F.T. Matthew, W.M. David, Steam pyrolysis activation of wood char for superior odorant removal, Carbon 41 (2003) 2195–2202.

[8] P.K. Malik, Use of activated carbons prepared from saw dust and rice-husk for adsorption of acid dyes: a case study of acid yellow 36, Dyes Pigments 56 (2003) 239–249.

[9] P.K. Malik, Dye removal from wastewater using activated carbon developed from sawdust: adsorption equilibrium and kinetics, J. Hazard. Mater. B113 (2004) 81–88.

[10] Q. Gan, S.J. Allen, R. Matthews, Activation of waste MDF sawdust charcoal and its reactive dye adsorption characteristics, Waste Manage. 24 (2004) 841–848.

[11] K. Kadirvelu, M. Kavipriya, G. Karthika, M. Radhika, N. Vennilamani, S. Pattabhi, Utilization of various agricultural wastes for activated carbon preparation and application for the removal of dyes and metal ions from aqueous solutions, Bioresour. Technol. 87 (2003) 129–132.

[12] V.K. Garg, M. Amita, R. Kumar, R. Gupta, Basic dye (methylene blue) removal from simulated wastewater by adsorption using Indian rosewood sawdust: a timber industry waste, Dyes Pigments 63 (2004) 243–250.

[13] V.K. Garg, G. Renuka, Y. Anu Bala, K. Rakesh, Dye removal from aqueous solution by adsorption on treated sawdust, Bioresour. Technol. 89 (2003) 121–124.

[14] V. Sivanandan Achari, T.S. Anirudhan, Phenol removal from aqueous systems by sorption on jackwood sawdust, Indian J. Chem. Technol. 2 (1995) 137–141.

[15] S.D. Khattri, M.K. Singh, Adsorption of basic dyes from aqueous solution by natural adsorbent, Indian J. Chem. Technol. 5 (1999) 230–234.

[16] C. Srinivasakannan, M.Z. Abu Bakar, Production of activated carbon from rubberwood sawdust, Biomass Bioenergy 27 (2004) 89–96.

[17] L.J. Yu, S.S. Shukla, K.L. Dorris, A. Shukla, J.L. Margrave, Adsorption of chromium from aqueous solution by maple sawdust, J. Hazard. Mater. B 100 (2003) 53–63.

[18] H. Benaddi, T.J. Bandosz, J. Jagiello, J.A. Schwarz, J.N. Rouzaud, D. Legras, F. Beguin, Surface functionality and porosity of activated carbons obtained from chemical activation of wood, Carbon 38 (2000) 669–674.

[19] V. Minkova, M. Razvigorova, E. Bjornbom, R. Zanzi, T. Budinova, N. Petrov, Effect of water vapour and biomass nature on the yield and quality of the pyrolysis products from biomass, Fuel Process. Technol. 70 (2001) 53–61.

[20] V.K. Garg, R. Kumar, G. Renuka, Removal of malachite green dye from aqueous solution by adsorption using agro-industry waste: a case study of *Prosopis cineraria*, Dyes Pigments 62 (2004) 1–10.

[21] M. Satish, B.C. Vanraj, L.M. Manocha, Porosity development on activation of char from dry and wet babbool wood, Carbon Sci. 3 (2002) 133–141.

[22] P.M. Satya Sai, J. Ahmed, K. Krishnaiah, Production of activated carbon from coconut shell char in a fluidized bed reactor, Ind. Eng. Chem. Res. 36 (1997) 3625–3630.

[23] A. Linares-Solano, L.C. Salinas-Martínez, D. Cazorla-Amorós, I. Martín-Gullón, Porosity development during CO_2 and steam activation in a fluidized bed reactor, Energy Fuels 14 (2000) 142–149.

[24] W.M.A.W. Daud, W.S.W. Ali, Comparison on pore development of activated carbon produced from palm shell and coconut shell, Bioresour. Technol. 93 (2004) 63–69.

[25] A. Aygün, S. Yenisoy-Karakaş, I. Duman, Production of granular activated carbon from fruit stones and nutshells and evaluation of their physical, chemical and adsorption properties, Microporour Mesoporous Mater. 66 (2003) 189–195.

[26] Y. Guo, K. Yu, Z. Wang, H. Xu, Effects of activation conditions on preparation of porous carbon from rice husk, Carbon 41 (2000) 1645–1687.

[27] Y. Guo, S. Yang, W. Fu, J. Qi, R. Li, Z. Wang, H. Xu, Adsorption of malachite green on micro- and mesoporous rice husk-based active carbon, Dyes Pigments 56 (2003) 219–229.

[28] ASTM, Standard Test Method for Determination of Iodine Number of Activated Carbon, D 4607-86, pp. 384–387.

[29] BIS, Determination of Decolorizing Power, IS: 877-1977, pp. 9–10.

[30] F. Banat, S. Al-Asheh, L. Al-Makhadmeh, Evaluation of the use of raw and activated date pits as potential adsorbents for dye containing waters, Process. Biochem. 39 (2003) 193–202.

[31] M.F.R. Pereira, S.F. Soares, J.J.M. Órfão, Adsorption of dyes on activated carbons: influence of surface chemical groups, Carbon 41 (2003) 811–821.

[32] A.C. Chao, S.S. Shyu, Y.C. Lin, F.L. Mi, Enzymatic grafting groups on to chitosan-to confer on chitosan the property of a cationic dye adsorbent, Bioresour. Technol. 91 (2004) 157–162.

[33] A. Bhatnagar, A.K. Jain, A comparative adsorption study with different industrial wastes as adsorbents for the removal of cationic dyes from water, J. Colloid Interface Sci. 281 (2005) 49–55.

[34] S. Netpradit, P. Thiravetyan, S. Towprayoon, Evaluation of metal hydroxide in a fixed-bed column system, Water Res. 38 (2004) 71–78.

[35] G.M. Walker, L.R. Weatherley, Adsorption of acid dyes on to granular activated carbon in fixed beds, Water Res. 31 (1997) 2093–2101.

[36] G.S. Bohart, E.Q. Adams, Some aspects of the behavior of charcoal with respect to chlorine, J. Am. Chem. Soc. 42 (1920) 523–544.

[37] R.A. Hutchins, New method simplifies design of activated carbon systems, Chem. Eng. 80 (1973) 133–138.

[38] G. McKay, M.J. Bino, Fixed bed adsorption for the removal of pollutants from water, Environ. Pollut. 66 (1990) 33–53.